THE JOURNAL OF BIOLOGICAL CHEMISTRY VOL. 281, NO. 11, pp. 7237–7243, March 17, 2006

Smoothened Regulates Activator and Repressor Functions of Hedgehog Signaling via Two Distinct Mechanisms*

Received for publication, September 15, 2005, and in revised form, December 21, 2005 Published, JBC Papers in Press, January 19, 2006, DOI 10.1074/jbc.M510169200

Stacey K. Ogden[‡], David J. Casso[§], Manuel Ascano, Jr.[‡¶], Mark M. Yore[‡], Thomas B. Kornberg[§], and David J. Robbins[‡1]

From the [‡]Department of Pharmacology and Toxicology, Dartmouth Medical School, Hanover, New Hampshire 03755, the [§]Department of Biochemistry and Biophysics, University of California, San Francisco, California 94143, and the [¶]Department of Molecular Genetics Graduate Program, University of Cincinnati Medical Center, Cincinnati, Ohio 45267

The secreted protein Hedgehog (Hh) plays an important role in metazoan development and as a survival factor for many human tumors. In both cases, Hh signaling proceeds through the activation of the seven-transmembrane protein Smoothened (Smo), which is thought to convert the Gli family of transcription factors from transcriptional repressors to transcriptional activators. Here, we provide evidence that Smo signals to the Hh signaling complex, which consists of the kinesin-related protein Costal2 (Cos2), the protein kinase Fused (Fu), and the *Drosophila* Gli homolog cubitus interruptus (Ci), in two distinct manners. We show that many of the commonly observed molecular events following Hh signaling are not transmitted in a linear fashion but instead are activated through two signals that bifurcate at Smo to independently affect activator and repressor pools of Ci.

In *Drosophila*, Hh-mediated target gene activation is thought to be a two-step process involving stabilization of Ci[2] and an as yet uncharacterized activation step that converts Ci to a transcriptional activator (1–6). In the absence of Hh, Ci is converted to a partially proteolyzed repressor protein, Ci_{75} (1), through a process involving the proteasome and priming phosphorylation by a cast of protein kinases including glycogen synthase kinase 3β, casein kinase I, and protein kinase A (7–14). Binding of Hh to its transmembrane receptor Patched (Ptc) activates Smo, promoting its phosphorylation by the same kinases that prime Ci for processing (12–14). Hh also triggers Smo accumulation at the plasma membrane (15), where it is believed to attenuate Ci to Ci_{75} processing and to trigger Ci activation (reviewed in Ref. 16). Hh-mediated activation of the Cos2, Fu, and Ci containing Hedgehog signaling complex (HSC) is thought to correlate with phosphorylation of Fu and Cos2 and the release of HSC components from Cos2-mediated membrane and microtubule associations (17–20). Although microtubule release and Cos2/Fu phosphorylation are considered to be requisite steps in the stabilization and subsequent activation of Ci, a number of studies in various genetic backgrounds have noted an incomplete correlation between Ci protein stabilization and Ci transcriptional activity (4, 5, 21, 22).

We and others (23–26) have reported that the cargo domain of Cos2 forms an association with Smo that is necessary for Hh-mediated Ci activation. This likely occurs through Hh-mediated Smo stabilization that facilitates additional HSC to associate with Smo through Cos2-mediated tethering (23). This phenomenon is somewhat contrary to our observation that, following Hh activation, the bulk of Cos2 releases from cellular membranes (27), whereas Cos2 bound to Smo accumulates on the plasma membrane (15, 23, 26). Thus, we targeted the Cos2-Smo association to better understand these seemingly conflicting events. We were able to modulate the Cos2-Smo association by overexpressing the Cos2 cargo domain and show that this domain can functionally separate the traditional read-outs of Hh pathway activation. We separate Fu and Cos2 hyperphosphorylation, Ci stabilization, and Cos2 membrane release from Smo accumulation and target gene activation *in vitro* and *in vivo*. Our results suggest that Smo regulates two arms of the Hh pathway, repression and activation, independently of each other and that this regulation can be functionally separated through targeting the Cos2-cargo Smo interaction.

MATERIALS AND METHODS

DNA Constructs—Act-renilla was constructed by subcloning *Renilla* from the *pRL-TK* plasmid (Promega) into *pAct 5.1A* (Invitrogen) via ScaI and BsrbI restriction sites. *pAct 5.1 ci* was generated by subcloning *ci* from *pUAS-ci* (1) via KpnI restriction sites. *pAct 5.1 3x HA-CSBD* was generated by PCR amplifying base pairs 3001–3601 of *Cos2* cDNA (corresponding to amino acids 1001–1201) with primers that introduce BglII sites flanking the *Cos2* coding sequence. PCR products were cloned into *pZero* (Invitrogen) then subcloned via the BglII sites into *pAc5.1A* (Invitrogen) in-frame with an engineered 3× HA epitope tag. Because of its small size, a nuclear export sequence was added to the carboxyl terminus of the HA-carboxyl-terminal Smo binding domain (CSBD) construct to prevent passive nuclear diffusion. An HIV-1 reverse nuclear export sequence linker (5′-GATCCCTTCAGCTTC-CACCACTTGAGCGACTTACCCCTA) (28) was inserted in-frame 3′ of the CSBD coding sequence in the *pAct 5.1 HA-CSBD* plasmid. CSBD and CSBD-nuclear export sequence expressed at similar levels and had similar effects on Hh signaling by the *ptc* reporter assay and analysis of Hh-induced Fu and Cos2 shifts (data not shown). *pAc5.1-GFP* was generated by PCR amplifying *EGFP* from *pEGFP* (Clontech) with primers introducing a BglII restriction site 5′ and a BamHI site 3′ and cloned into the *pZero* vector (Invitrogen). *EGFP* was liberated from *pZero* via BglII/BamHI digest and subcloned into *pAc5.1A* at the existing BamHI site. Ligation inactivates the 5′-BglII/BamHI site but leaves the 3′-site intact for cloning purposes. CSBD-GFP was generated by subcloning *CSBD* from *pZero* into *pAc5.1-GFP* 3′ of *EGFP* via the intact BamHI site. *pAct 5.1 myc-smo* was generated by PCR amplification of *myc-smo* from *pRM-myc-smo* (gift from J. Hooper) with primers that introduced

* This work was supported by National Institutes of Health Grants CA82628 (to D. J. R.) and T32-ES07250-14 (to S. K. O. and M. A.). The costs of publication of this article were defrayed in part by the payment of page charges. This article must therefore be hereby marked "*advertisement*" in accordance with 18 U.S.C. Section 1734 solely to indicate this fact.

[1] To whom correspondence should be addressed: Dept. of Pharmacology and Toxicology, Dartmouth Medical School, HB 7650 Remsen, Hanover, NH, 03755-7650. Tel.: 603-650-1716; Fax: 603-650-1129; E-mail: David.J.Robbins@dartmouth.edu.

[2] The abbreviations used are: Ci, *cubitus interruptus*; HSC, Hedgehog signaling complex; HA, hemagglutinin; GFP, green fluorescent protein; EGFP, enhanced GFP; RNAi, RNA interference; CSBD, Cos2 carboxyl-terminal Smo binding domain; Hh, Hedgehog; HSC-R, HSC repression; HSC-A, HSC activation; UAS, upstream activator sequence.

HindIII sites 5′ and 3′ of the *myc-smo* coding sequence. The *myc-smo* PCR product was cloned into a multiple cloning site shuttling vector via the HindIII sites, then liberated and cloned into *pAc5.1A* using EcoRV and NotI restriction sites. *Ptc-luciferase* was provided by P. Beachy (7), *pUAS-smo-GFP* was provided by M. Scott (29), *pUAS-smoC* was provided by J. Hooper (30).

Fly Strains and Transgenes—*pUAS-HA-CSBD* was generated by liberating *HA-CSBD* from *pAc5.1-HA-Cos2 SBD* and introduced into *pUAST* (31) using KpnI and XbaI restriction sites. Germ line transformation was performed by the Duke University Molecular Biology Core using standard protocols. When *HA-CSBD* was crossed into *ptc*-GAL4, CSBD expression was confirmed by Western blot analysis of wing imaginal disc lysates (data not shown). To generate *smo* RNAi-expressing flies, a 1012-base-pair portion of the Smo coding region one codon 3′ of the initiating methionine was amplified with 5′-(TTTTCTAGAGCAGTACTTAAACTTTCCGC) and 3′-(TTTTCTAGAAAGATTTTCACCGGCTGTAGG) primers. Two copies of the amplified sequence were subcloned into the P-element vector *pWIZ* (32) in a tail-to-tail fashion so that a double stranded RNA of the *smo* transcript could be expressed under control of the GAL4 system. Germ line transformation was performed as described (33). *Dpp-LacZ* flies were provided by D. Kalderon. Fly stocks were maintained on standard yeast-cornmeal agar at room temperature. Experimental crosses were preformed at 29 °C.

Cell Culture and Assays—All cell transfections were performed using Cellfectin reagent (Invitrogen) per the manufacturer's instructions. For all assays, Hh was provided via transfection of a full-length Hh expression vector (pAct FL-Hh). The *ptc* reporter assay and *ptc-luciferase* reporter construct have been previously described (7, 24). *ptc-luciferase* activity was normalized to expression of an *act-renilla* control plasmid. Reporter assays were preformed a minimum of three times, in duplicate. Error bars represent S.E. For Western blot analysis, cells were lysed in 1% Nonidet P-40 lysis buffer (150 mM NaCl, 50 mM Tris, 50 mM NaFl, pH 8.0) and cleared of nuclei by a 2000 × *g* spin. Postnuclear lysates were blotted using anti-HA to detect CSBD (Covance), anti-Ci_{155} (2A1), anti-Ci_{75} (CiN, gift from R. Holmgren), anti-Fu Hinge (20, 34), anti-Cos2 (5D6), anti-Ptc (47H8, gift from R. Johnson), anti-Smo,[3] anti-myc (Covance) and anti-Kinesin (Cytoskeleton, Inc.) antibodies. For membrane binding assays cells were lysed hypotonically by Dounce homogenization in HKB (20 mM Hepes, 10 mM KCl, pH 7.9). To prepare membrane pellets, postnuclear lysates were centrifuged for 30 min at 100,000 × *g* in a table-top ultracentrifuge. Membrane pellets were resuspended by homogenization in HLB + 1% Nonidet P-40. For all experiments, DNA content is as follows: 1× is 250 ng, 2× is 500 ng, and 4× is 1 μg. The Hh expression vector was transfected at a ratio of 250 ng of DNA to every $3E^6$ cells. To determine the transfection efficiency of CSBD-GFP, two fields of cells were counted in bright field and fluorescent field. Averaged GFP and non-GFP cell numbers were used to determine the percent of cells expressing GFP.

Immunoflourescence and Microscopy—Wing imaginal discs were collected and immunostained using standard methods, as described previously (24). Smo immunostain was preformed as described recently (13). Discs and/or S2 cells were immunostained using anti-Ci (2A1), anti-HA (Genetex), anti-En (gift from C. Goodman) and anti-Smo (11F1) primary antibodies and appropriate Alexa-Fluor-conjugated secondary antibodies (Molecular Probes). S2 cells used for immunolocalization assays were plated on Con A-treated slides and immunostained as previously described (24, 35). Percentages of cells demonstrating punctate or diffuse Smo localizations were determined by randomly counting 200–250 Smo-staining cells across three separate experiments. Confocal images of imaginal discs and S2 cells were collected using a Leica TCS SP confocal laser scanning microscope and processed using Adobe Photoshop 6.0. Imaginal disc images were collected using a 20× objective at 1024 × 1024 pixel resolution. S2 cell images were collected using a 100× oil-immersion objective at 1024 × 1024 pixel resolution. For wing images, wings were mounted using DPX mounting medium (Electron Microscopy Services) and imaged using a Leica M212 dissecting scope with an Optronics DEI 750 camera and Metaview software. Images were processed using Adobe Photoshop 6.0

RESULTS

Previous studies have demonstrated that the primary interaction between Smo and Cos2, which appears to be required for Hh activation, is through the Cos2 carboxyl-terminal cargo domain (23, 25, 26). Thus, we tested whether overexpression of the Cos2 CSBD could decrease activation of the Hh target gene *ptc* in Clone-8 (Cl8) cells. We found that CSBD is a strong inhibitor of Hh-mediated activation of a *ptc-luciferase* reporter construct, capable of decreasing maximal Hh activation by nearly 80% (Fig. 1*A*). CSBD-mediated inhibition can be rescued by overexpression of Ci, consistent with CSBD functioning upstream of Ci (Fig. 1*B*).

A construct expressing the carboxyl-terminal tail of Smo (SmoC) affects both activation and repression of Hh signaling: SmoC promotes low level signaling in the absence of Hh and decreases signaling in Hh-stimulated cells (30). We were surprised to find that although both SmoC and CSBD inhibit Hh-mediated target gene activation (Fig. 1*A*), they differ in their effects on Ci, Cos2, and Fu. In response to Hh, full-length Ci_{155} is stabilized, resulting in a decrease of the proteolyzed repressor form, Ci_{75} (Fig. 1*C*, compare *lane 1* with *4* and *7* with *10*). SmoC has previously been demonstrated to alter this Ci_{155}/Ci_{75} ratio *in vivo*, such that levels of Ci_{155} are decreased in Hh-responding cells (30). Accordingly, expression of SmoC *in vitro* decreases the Hh-induced stabilization of Ci_{155}, resulting in a decreased Ci_{155}/Ci_{75} ratio in Hh-stimulated cells (Fig. 1*C*, compare *lane 10* with *lanes 11* and *12*). Interestingly, CSBD does not affect the ratio of Ci_{155}/Ci_{75} in Hh-stimulated cells (Fig. 1*C*, compare *lane 4* with *5* and *6*). Further, although SmoC attenuates Hh-induced Fu and Cos2 hyperphosphorylation, CSBD has no effect on this phosphorylation (Fig. 1*C*, compare *lanes 4–6* with *10–12*). To confirm that the inability of CSBD to attenuate Fu and Cos2 phosphorylation or Ci stabilization were not the result of a population effect of non-CSBD-expressing cells, we expressed a GFP-tagged CSBD construct in Cl8 cells and calculated the approximate transfection efficiency. We then analyzed the lysates for Fu, Cos2, and Ci and found that even when transfection efficiency of GFP-CSBD approaches 80%, Hh-induced Fu and Cos2 phosphorylation and Ci stabilization are maintained (data not shown). GFP-CSBD represses reporter assay target gene activation to the same extent as HA-CSBD (data not shown). These results suggest that CSBD disrupts Hh signaling through a mechanism distinct from that of SmoC. CSBD appears to target a specific pool of Cos2-Smo complexes involved in the activation of Ci, but not in its stabilization, or the hyperphosphorylation of Fu and Cos2. SmoC, however, functions as a more general inhibitor, targeting all of these Hh-induced processes.

To confirm that CSBD could repress the Hh-mediated activation of an endogenous gene, we overexpressed CSBD in Cl8 cells in the presence or absence of Hh. We found that, as with the *ptc* reporter construct, CSBD expression resulted in a significant reduction in Hh-activated expression of endogenous *ptc*, without affecting Hh-induced Fu

[3] D. J. Casso and T. B. Kornberg, unpublished work.

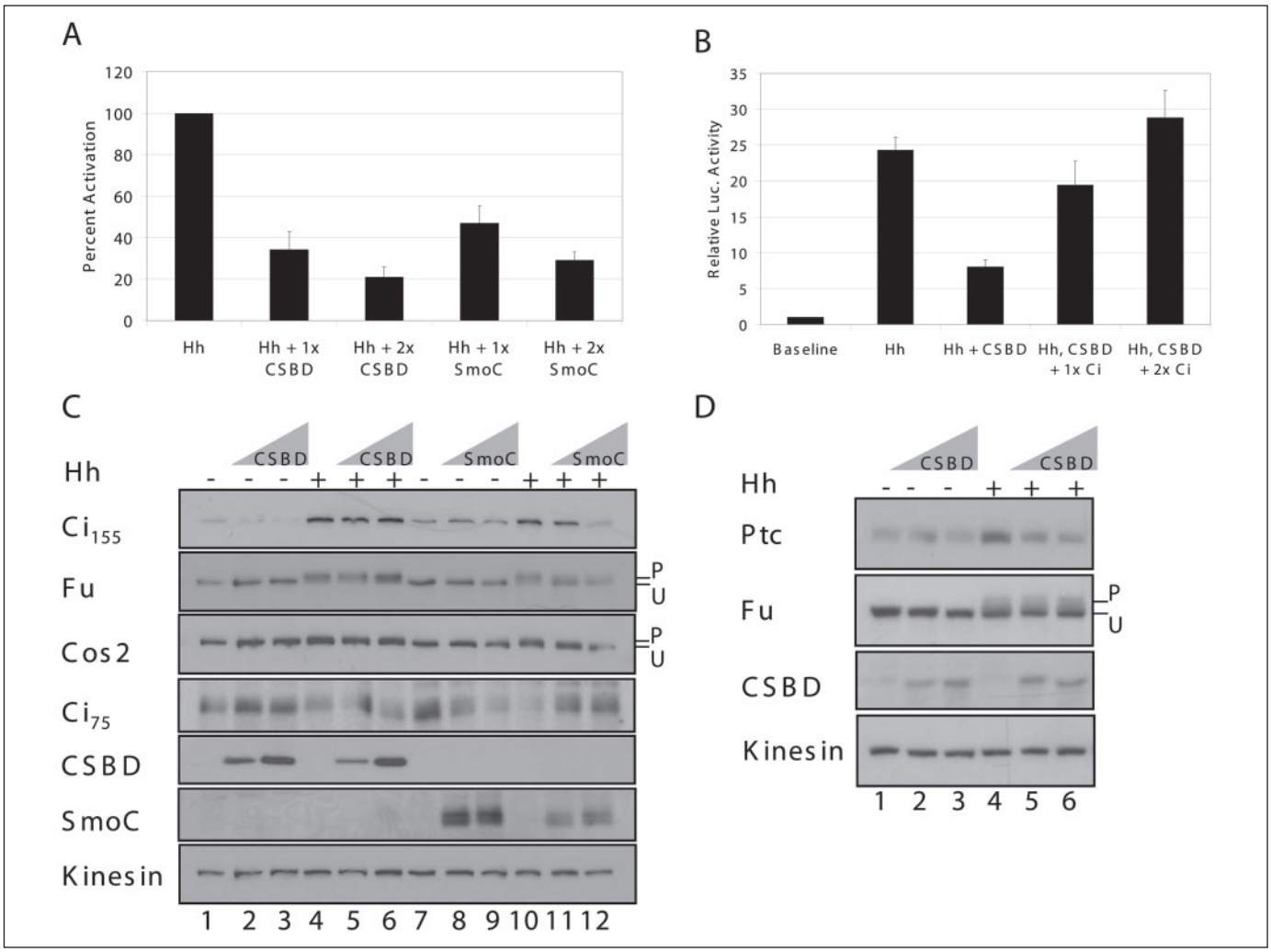

FIGURE 1. **CSBD uncouples target gene activation from Ci stabilization and Fu/Cos2 hyperphosphorylation.** *A*, CSBD is a strong inhibitor of Hh-mediated target gene activation. CI8 cells were transfected with a *ptc-luciferase* reporter construct and increasing amounts of plasmids expressing CSBD, SmoC, or empty vector control, in the presence or absence of a Hh expression vector. Percent expression relative to maximal Hh activation is indicated. *ptc-luciferase* expression levels were normalized to an *act-renilla* transfection control. *Error bars* indicate S.E. For all experiments, 1× corresponds to 250 ng of transfected DNA and 2× corresponds to 500 ng. *B*, Ci reverses CSBD-mediated repression. CI8 cells were co-transfected with plasmids expressing Hh, CSBD and increasing amounts of Ci, or empty vector control. Relative *ptc-luciferase* expression levels were normalized to an *act-renilla* control. *Error bars* indicate S.E. For all experiments, 1× corresponds to 250 ng of transfected DNA and 2× corresponds to 500 ng. *C*, CSBD and SmoC have different effects on the molecular markers of Hh activation. CI8 cells were co-transfected with increasing amounts of plasmids expressing CSBD (250 and 500 ng) or SmoC (250 and 500 ng) in the presence or absence of Hh. DNA content was normalized with empty vector. 1% Nonidet P-40 cell lysates were immunoblotted for Ci_{155}, Fu, Cos2, Ci_{75}, CSBD, SmoC, and kinesin. Hyperphosphorylated forms of Cos2/Fu are marked with *bars* (*P*, phosphorylated; *U*, unphosphorylated). The results shown are representative of at least three independent experiments. *D*, CSBD inhibits Hh-mediated activation of endogenous *ptc*. CI8 cells were transfected with increasing amounts of a plasmid expressing CSBD in the presence or absence of Hh. 1% Nonidet P-40 cell lysates were immunoblotted for Ptc, Fu, CSBD, and kinesin. Hyperphosphorylated forms of Fu are marked with *bars* (*P*, phosphorylated; *U*, unphosphorylated). The results shown are representative of at least three independent experiments.

phosphorylation (Fig. 1*D*, compare *lane 1* with *4* and *lane 4* with *5* and *6*). Semiquantitative reverse transcription PCR analysis confirmed that repression occurs at the level of transcription (data not shown).

To determine whether CSBD could exhibit similar effects *in vivo* we expressed CSBD in *Drosophila* wing imaginal discs using the UAS-GAL4 system. We analyzed the wings of transgenic flies, as disrupted Hh signaling in the wing imaginal disc results in specific wing patterning defects in the adult (reviewed in Refs. 36 and 37). Transgenic flies expressing CSBD under the control of the *ptc*-GAL4 driver demonstrate decreased spacing between LV3 and LV4 (Fig. 2, compare *A* with *B*) and proximal LV3-4 fusions (Fig. 2*B*, *arrow*), indicative of disrupted Hh signaling. Expression of CSBD in a Smo-sensitized background resulted in a robust enhancement of the Smo phenotype (Fig. 2, compare *D* with *B*). Smo-sensitized flies express a Smo double stranded RNA (Smo-RNAi), which primes them for the detection of factors that affect Smo function.[4] Smo-RNAi flies do not demonstrate increased lethality but do show modest proximal fusions of LV3-4 (Fig. 2*C*, *arrow*) with normal LV3-4 spacing. The expression of CSBD in Smo-RNAi flies results in a near lethal phenotype. Approximately 4% of the flies escape lethality but demonstrate significantly decreased LV3-4 spacing and more pronounced LV3-4 fusions (Fig. 2*D*, *arrows*). These results are consistent with Smo being the *in vivo* target of CSBD.

Our biochemical results suggest that CSBD can alter Hh target gene activity without affecting Ci stabilization. Accordingly, analysis of late third instar wing imaginal discs demonstrates that although the Smo RNAi-CSBD wings show strong Hh phenotypes, discs from CSBD expressing Smo-RNAi flies reveal a near normal Ci protein gradient (Fig. 2, compare *E* with *F′*, *arrows*). CSBD appears to have no observable

[4] D. J. Casso and T. B. Kornberg, unpublished data.

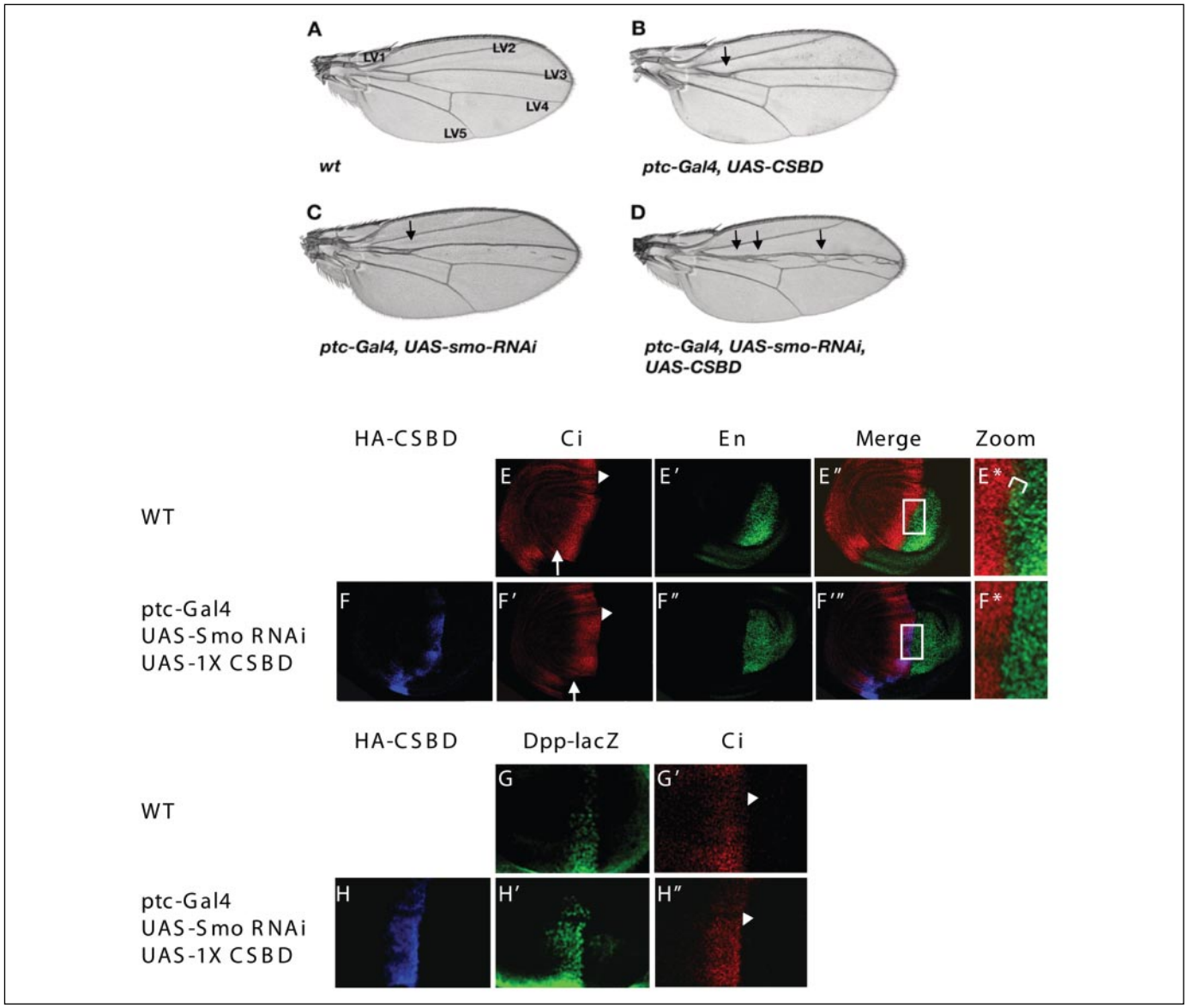

FIGURE 2. **CSBD uncouples target gene activation from Ci stabilization *in vivo*.** *A–D*, CSBD overexpression results in disruption of Hh signaling. Wings from wild type flies demonstrate normal patterning of longitudinal veins (*LV*) 1–5 (*A*). Wings from ptc-GAL4;UAS-HA-CSBD flies demonstrate mild LV3-LV4 fusions (*arrow*). Wings from *ptc*-GAL4 (*B*), UAS-*Smo RNAi* flies (*C*) demonstrate a mild fusion of LV3-LV4 (*arrow*). Overexpression of CSBD in Smo-RNAi flies triggers a near lethal phenotype. Wings of surviving *ptc*-GAL4, UAS-*Smo RNAi*; UAS-*CSBD* flies (*D*) demonstrate significantly decreased LV3–4 spacing and more severe LV3–4 fusions (*arrows*), indicating an enhanced loss of normal Hh signaling. *E–F*, CSBD disrupts Hh target gene activation without affecting Ci protein stabilization. Late third instar wing imaginal discs from wild type (*E*) and *ptc*-GAL4, UAS-*Smo RNAi*; UAS-*HA-CSBD* (*F*) flies were immunostained with anti-HA (*blue*, *F*), anti-Ci (*red*, *E* and *F*), and anti-En (*green*) antibodies as indicated. CSBD has little effect on Hh activated Ci stabilization in cells 3–8 cell diameters from the A/P border (*arrow*) but does affect Ci* (*arrowheads*) and anterior expression of the high level target gene *en* (F″ and F* *bracket*). For all discs, anterior is toward the left and dorsal is toward the top. *G–H*, CSBD does not alter *dpp* expression. Late third instar wing imaginal discs from wild type (*G*) and p*tc*-GAL4, UAS-*Smo RNAi*; UAS-*HA-CSBD* (*H*) flies were immunostained with anti-HA (*blue*, *H*), anti-Ci (*red*, *G′* and *H″*), and anti β-galactosidase (*green*, *G* and *H′*) antibodies as indicated. Although CSBD does alter Ci* expression in cells immediately adjacent to the A/P border (*arrowheads*), expression of the low level target gene *dpp-lacZ* is not affected. For all discs, anterior is toward the left and dorsal is toward the top.

effects on the normal Hh-induced stabilization of Ci occurring 3–8 cell diameters away from the anterior/posterior (A/P) border (Fig. 2, compare *E* with *F′*, *arrow*). However, the zone of highest level Ci activity, termed Ci*, and evidenced by decreased Ci staining immediately adjacent to the A/P border, is lost (Fig. 2, *E* and *F′*, *arrowheads*). Accordingly, expression of the Ci* target gene *engrailed* (*en*) in anterior compartment cells immediately adjacent to the A/P border is lost in CSBD-expressing discs (Fig. 2, compare *E** with *F**, *brackets*). Expression of the high level Hh target gene *ptc* is also decreased by CSBD expression (data not shown). Conversely, CSBD does not have a significant effect on expression of the low level target gene *decapentaplegic* (*dpp*) when expressed under control of the *ptc*-Gal4 (Fig. 2, compare *G* with *H′*) or *apterous*-GAL4 drivers (data not shown). These results are consistent with CSBD not affecting the Ci_{155}/Ci_{75} ratio in Hh-responding cells, in that *dpp* expression is derepressed through Hh-induced attenuation of Ci_{75} processing (5). Taken together with our biochemical analyses, these *in vivo* results support the hypothesis that CSBD specifically inhibits an activating pool of the HSC involved in Ci activation but has little effect on the Hh-induced attenuation of Ci_{75} processing.

Cos2 targets the HSC to vesicular membranes, independently of Cos2-Smo association (27). Hh stimulates the release of the HSC from membranes concomitant with Cos2 and Fu hyperphosphorylation and Ci stabilization. To determine whether CSBD would affect the Hh-induced HSC membrane release, we expressed CSBD in Cl8 cells, in the

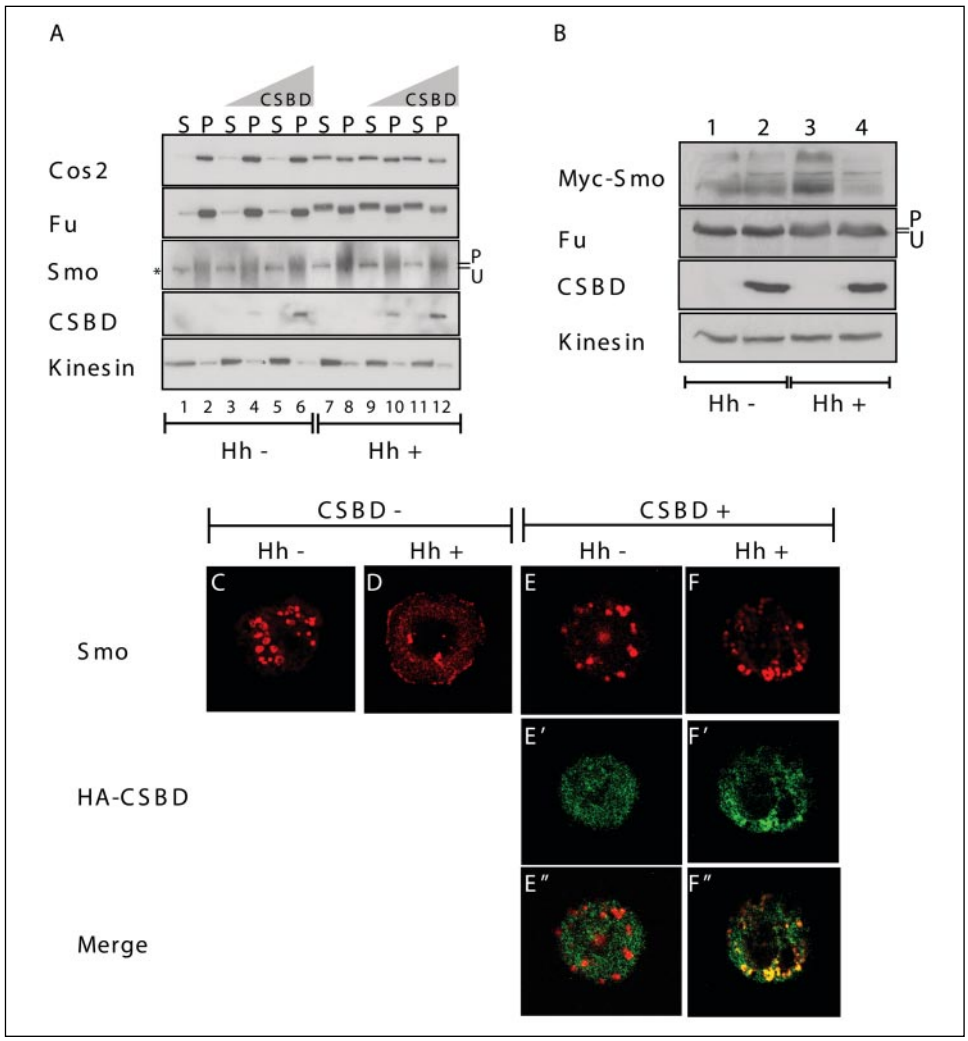

FIGURE 3. **CSBD blocks Ci activation by targeting Smo.** *A*, HSC membrane release is unaffected by CSBD. Cl8 cells were co-transfected with plasmids expressing increasing amounts of HA-CSBD (*lanes 3–6* and *9–12*; 500 ng (*lanes 3*, *4*, *9*, *10*) and 1 μg (*lanes 5*, *6*, *11*, *12*) CSBD expression vector) in the presence (*lanes 7–12*) or absence (*lanes 1–6*) of a Hh expression vector. Hypotonic cell lysates were fractionated, and the resulting membrane pellets (*P*) and cytosolic soluble fractions (*S*) were analyzed by immunoblot. *U*, unphosphorylated; *P*, phosphorylated. *, the band appearing in the *S* fraction in the Smo blot is either a nonspecific band or a minor membrane contamination in the soluble fraction, as it does not reproducibly appear in this assay. The results shown are representative of a minimum of three independent experiments. *B*, CSBD inhibits Hh-mediated Smo accumulation in S2 cells. Myc-Smo was expressed in S2 cells plus or minus HA-CSBD (1 μg, *lanes 2* and *4*) and Hh expression vector (*lanes 3* and *4*). 1% Nonidet P-40 cell lysates were analyzed by immunoblot analysis. *C–F*, CSBD alters Hh-mediated Smo subcellular relocalization. S2 cells transfected with 1 μg of a plasmid expressing Smo in the presence (*E* and *F*) or absence (*C* and *D*) of 1 μg of HA-CSBD expression vector and Hh expression vector (*D* and *F*) were plated on concanavalin A-treated slides and immunostained for Smo (*red*) and HA-CSBD (*green*).

presence or absence of Hh, and assayed for membrane association. In the absence of Hh stimulation the majority of Cos2 and Fu associate with cellular membranes both plus and minus CSBD expression (Fig. 3*A*, *P* fractions). In response to Hh, a significant amount of HSC releases from membranes (compare *lanes 1* and *2* with *7* and *8*, compare *S* fractions with *P* fractions). This membrane release is unaffected by CSBD expression (*lanes 9–12*, *S* fractions), suggesting that CSBD does not disrupt Hh activation through blocking HSC membrane release. However, expression of CSBD decreases Hh-induced Smo stabilization and phosphorylation (Fig. 3*A*, compare *lane 8* with *lanes 10* and *12*, *P* fractions), consistent with CSBD targeting the rate-limiting step in Hh activation, Smo stabilization (15, 23, 26).

Hh-mediated stabilization and activation of Smo correlates with changes in its subcellular localization (15). It has been suggested that Cos2 may play a role in Hh-activated Smo movement (29, 38). Thus, we wanted to determine whether CSBD disrupts Smo activation and/or stabilization through alteration of its subcellular localization. Because of their larger size, we found that Schneider 2 (S2) cells provide greater resolution for analyzing subcellular localization than Cl8 cells in immunofluorescence assays. To confirm that overexpressed Smo in S2 cells would behave in a manner similar to endogenous Smo in Cl8 cells, we expressed Myc-Smo in S2 cells in the presence or absence of CSBD and Hh and then analyzed lysates for Hh-induced Myc-Smo accumulation (Fig. 3*B*). In the absence of Hh, CSBD has little effect on Myc-Smo protein stability (Fig. 3*B*, compare *lane 1* with *2*). However, we found that, as with endogenous Smo in Cl8 cells, the Hh-induced stabilization of epitope-tagged Smo is dramatically reduced by CSBD (compare *lane 3* with *4*).

To examine whether CSBD expression altered Hh-stimulated Smo relocalization to the plasma membrane, we transfected S2 cells with a plasmid expressing Smo in the presence or absence of CSBD and then analyzed Hh-induced Smo relocalization (Fig. 3, *C–F*). In the absence of Hh, Smo localizes to discrete puncta in ~75% of cells (Fig. 3*C*). The remaining 25% of cells demonstrate a diffuse localization pattern (data not shown). In response to Hh, the population of cells demonstrating a diffuse Smo localization shifts such that ~70% of the cells now show a more diffuse Smo distribution with evident plasma membrane localization (Fig. 3*D*). We noticed a striking change in Hh-activated Smo relocalization when CSBD was co-expressed (Fig. 3, compare *F* with *D*). Instead of an obvious shift to a more diffuse and plasma membrane localization pattern, Smo remains punctate in ~65% of Hh-stimulated cells. We concluded that the Cos2 cargo domain-Smo interaction is necessary for the translocation of Smo, with HSC components, to the plasma membrane to activate Ci.

DISCUSSION

In this work, we have demonstrated that targeting the association between Smo and the Cos2 cargo domain functionally separates the known molecular markers of the Hh pathway into two distinct categories: those events dependent on a direct association between the Cos2

cargo domain and Smo and those not dependent on this direct association. The Hh-induced readouts requiring direct Smo-Cos2 association include Smo phosphorylation, stabilization, and translocation to the plasma membrane, which facilitate intermediate to high level activation of Ci. Hh-induced Fu and Cos2 hyperphosphorylation, HSC relocalization from vesicular membranes to the cytoplasm, and Ci stabilization do not appear to require a direct Smo-Cos2 cargo domain association. Thus, although Smo is necessary for all aspects of Hh signaling (reviewed in Ref. 39), only the molecular events grouped with Ci activation appear to require direct association between Cos2 and Smo. *In vivo*, CSBD expression is also capable of attenuating Hh signaling. This observation is consistent with our *in vitro* observation that CSBD inhibits its critical requirement(s) for pathway activation (12, 13, 40).

We have previously proposed a model suggesting the existence of two independently regulated pools of HSC, one involved in pathway repression (HSC-R), and one involved in activation (HSC-A) (16). HSC-R is dedicated to priming Ci for processing into the Ci_{75} transcriptional repressor, whereas HSC-A is dedicated to activation of stabilized Ci_{155} in response to Hh. Here, we provide evidence that the effects of these two HSCs can be functionally separated by specifically targeting the interaction between Smo and the Cos2 cargo domain. Moreover, we identify distinct molecular markers for each HSC. We propose that in HSC-R, the membrane vesicle tethered Cos2 functions as a scaffold to recruit protein kinase A, glycogen synthase kinase 3β, and casein kinase I, which in turn phosphorylate Ci (40). Hyperphosphorylated Ci is then targeted to the proteasome by the F-box protein supernumerary limbs (Slimb), where it is converted into Ci_{75} (8, 23–26, 30, 38). In response to Hh, Fu and Cos2 are phosphorylated and dissociate from vesicular membranes and microtubules, which we suggest results in the attenuation of HSC-R function. This allows for the subsequent accumulation of full-length Ci. The mechanism by which HSC-R function is inhibited by Hh-activated Smo is not clear but appears to require the carboxyl-terminal tail of Smo and, by our analysis, appears to occur independently of a direct Smo-Cos2 cargo domain association. However, the direct Cos2-Smo association is critical for regulation of HSC-A. In the absence of Hh, HSC-A is tethered to vesicular membranes, through Smo, where it is kept in an inactive state. In the presence of Hh, Cos2 bound directly to Smo acts as a scaffold for the phosphorylation of Smo by protein kinase A, glycogen synthase kinase 3β, and casein kinase I. Phosphorylation of Smo triggers its stabilization and relocalization to the plasma membrane with HSC-A (12–14), where we propose that Ci is activated. Thus, Cos2 plays a similar role in both HSC-R and HSC-A. In the former case, coupling protein kinase A, glycogen synthase kinase 3β, and casein kinase I with Ci and, in the latter case, coupling the same protein kinases with the carboxyl-terminal tail of Smo (Fig. 4*A*).

An alternative interpretation of these data is that disruption of the Cos2 cargo domain-Smo association separates high and low level Hh signaling. It has been suggested that a second, low affinity Smo binding domain may reside within the coiled-coil domain of Cos2 (23, 25). Thus, high level signaling, where all aspects of the Hh pathway are activated may require both Cos2 interaction domains to be directly bound to Smo. In either scenario, HSC-R function would be regulated independently of HSC-A function.

We conclude that targeted disruption of Cos2 cargo domain-Smo binding by CSBD is able to functionally separate the activities ascribed to our two HSC model. This two-switch system is amenable to the formation of a gradient of Hh signaling activity across a field of cells, in that the relative activity of HSC-R to HSC-A is directly proportional to the level of Hh stimulation a cell receives (Fig. 4*B*). The opposing functional effects of the two complexes can then establish unique ratios of Ci_{75} to activated Ci, resulting in distinct levels of pathway activation on a per cell basis.

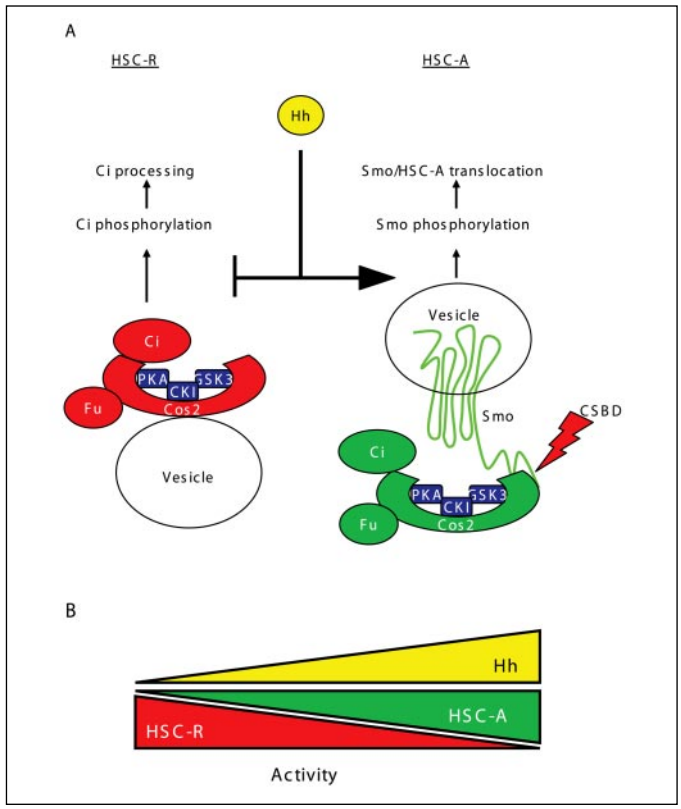

FIGURE 4. **A model for separation of activator and repressor functions of Hh signaling.** *A*, Cos2 functions as a scaffold in HSC-R and HSC-A. Hh attenuates HSC-R function by inhibiting Ci phosphorylation and its subsequent processing into a transcriptional repressor. Hh promotes the activity of HSC-A by stimulating the phosphorylation and stabilization of Smo, thereby allowing for the formation of additional Cos2-Smo complexes. Stabilized Smo translocates to the plasma membrane where it likely activates Ci. CSBD selectively inhibits HSC-A by blocking the relevant Cos2-Smo association. HSC-R is intact in the presence of CSBD, as its regulation by Hh does not depend on Cos2 cargo domain-Smo binding. *B*, model for the reciprocal activity of HSC-A and HSC-R in response to Hh. High level Hh stimulation promotes the high activity of HSC-A and low level activity of HSC-R. As the level of Hh stimulation decreases, HSC-A action decreases and HSC-R activity becomes predominant.

Acknowledgments—We are grateful to P. Beachy, L. Lum, M. Scott, and J. Hooper for constructs and antibodies, D. Kalderon for dpp-LacZ flies, J. Witney for technical assistance, and members of the Robbins' laboratory for helpful discussions. We especially thank Y. Ahmed (DMS) for all helpful suggestions during the course of this work. We are grateful to the Dartmouth College Microscopy Core for their expert assistance.

REFERENCES

1. Aza-Blanc, P., Ramirez-Weber, F. A., Laget, M. P., Schwartz, C., and Kornberg, T. B. (1997) *Cell* **89,** 1043–1053
2. Sanchez-Herrero, E., Couso, J. P., Capdevila, J., and Guerrero, I. (1996) *Mech. Dev.* **55,** 159–170
3. Wang, Q. T., and Holmgren, R. A. (2000) *Development* (*Camb.*) **127,** 3131–3139
4. Ohlmeyer, J. T., and Kalderon, D. (1998) *Nature* **396,** 749–753
5. Methot, N., and Basler, K. (1999) *Cell* **96,** 819–831
6. Wang, G., Wang, B., and Jiang, J. (1999) *Genes Dev.* **13,** 2828–2837
7. Chen, C. H., von Kessler, D. P., Park, W., Wang, B., Ma, Y., and Beachy, P. A. (1999) *Cell* **98,** 305–316
8. Jiang, J., and Struhl, G. (1998) *Nature* **391,** 493–496
9. Price, M. A., and Kalderon, D. (1999) *Development* (*Camb.*) **126,** 4331–4339
10. Price, M. A., and Kalderon, D. (2002) *Cell* **108,** 823–835
11. Jia, J., Amanai, K., Wang, G., Tang, J., Wang, B., and Jiang, J. (2002) *Nature* **416,** 548–552
12. Apionishev, S., Katanayeva, N. M., Marks, S. A., Kalderon, D., and Tomlinson, A.

(2005) *Nat. Cell Biol.* **7,** 86–92
13. Jia, J., Tong, C., Wang, B., Luo, L., and Jiang, J. (2004) *Nature* **432,** 1045–1050
14. Zhang, C., Williams, E. H., Guo, Y., Lum, L., and Beachy, P. A. (2004) *Proc. Natl. Acad. Sci. U. S. A.* **101,** 17900–17907
15. Denef, N., Neubuser, D., Perez, L., and Cohen, S. M. (2000) *Cell* **102,** 521–531
16. Ogden, S. K., Ascano, M., Jr., Stegman, M. A., and Robbins, D. J. (2004) *Biochem. Pharmacol.* **67,** 805–814
17. Ramirez-Weber, F. A., Casso, D. J., Aza-Blanc, P., Tabata, T., and Kornberg, T. B. (2000) *Mol. Cell* **6,** 479–485
18. Robbins, D. J., Nybakken, K. E., Kobayashi, R., Sisson, J. C., Bishop, J. M., and Therond, P. P. (1997) *Cell* **90,** 225–234
19. Sisson, J. C., Ho, K. S., Suyama, K., and Scott, M. P. (1997) *Cell* **90,** 235–245
20. Stegman, M. A., Vallance, J. E., Elangovan, G., Sosinski, J., Cheng, Y., and Robbins, D. J. (2000) *J. Biol. Chem.* **275,** 21809–21812
21. Wang, Q. T., and Holmgren, R. A. (1999) *Development* (*Camb.*) **126,** 5097–5106
22. Alves, G., Limbourg-Bouchon, B., Tricoire, H., Brissard-Zahraoui, J., Lamour-Isnard, C., and Busson, D. (1998) *Mech. Dev.* **78,** 17–31
23. Lum, L., Zhang, C., Oh, S., Mann, R. K., von Kessler, D. P., Taipale, J., Weis-Garcia, F., Gong, R., Wang, B., and Beachy, P. A. (2003) *Mol. Cell* **12,** 1261–1274
24. Ogden, S. K., Ascano, M., Jr., Stegman, M. A., Suber, L. M., Hooper, J. E., and Robbins, D. J. (2003) *Curr. Biol.* **13,** 1998–2003
25. Jia, J., Tong, C., and Jiang, J. (2003) *Genes Dev.* **17,** 2709–2720
26. Ruel, L., Rodriguez, R., Gallet, A., Lavenant-Staccini, L., and Therond, P. P. (2003) *Nat. Cell Biol.* **5,** 907–913
27. Stegman, M. A., Goetz, J. A., Ascano, M., Jr., Ogden, S. K., Nybakken, K. E., and Robbins, D. J. (2004) *J. Biol. Chem.* **279,** 7064–7071
28. Fasken, M. B., Saunders, R., Rosenberg, M., and Brighty, D. W. (2000) *J. Biol. Chem.* **275,** 1878–1886
29. Zhu, A. J., Zheng, L., Suyama, K., and Scott, M. P. (2003) *Genes Dev.* **17,** 1240–1252
30. Hooper, J. E. (2003) *Development* (*Camb.*) **130,** 3951–3963
31. Brand, A. H., and Perrimon, N. (1993) *Development* (*Camb.*) **118,** 401–415
32. Lee, Y. S., and Carthew, R. W. (2003) *Methods* **30,** 322–329
33. Spradling, A. C., and Rubin, G. M. (1982) *Science* **218,** 341–347
34. Ascano, M., Jr., Nybakken, K. E., Sosinski, J., Stegman, M. A., and Robbins, D. J. (2002) *Mol. Cell Biol.* **22,** 1555–1566
35. Ascano, M., Jr., and Robbins, D. J. (2004) *Mol. Cell Biol.* **24,** 10397–10405
36. Crozatier, M., Glise, B., and Vincent, A. (2004) *Trends Genet.* **20,** 498–505
37. Ingham, P. W., and McMahon, A. P. (2001) *Genes Dev.* **15,** 3059–3087
38. Nakano, Y., Nystedt, S., Shivdasani, A. A., Strutt, H., Thomas, C., and Ingham, P. W. (2004) *Mech. Dev.* **121,** 507–518
39. Hooper, J. E., and Scott, M. P. (2005) *Nat. Rev. Mol. Cell Biol.* **6,** 306–317
40. Zhang, W., Zhao, Y., Tong, C., Wang, G., Wang, B., Jia, J., and Jiang, J. (2005) *Dev. Cell* **8,** 267–278